Structure and Properties of Drawn Tapes of High-Density Polyethylene/Ethylene Copolymer Blends. I

S. J. MAHAJAN,[1] B. L. DEOPURA,[1,*] and YIMIN WANG[2]

[1]Textile Technology Department, Indian Institute of Technology, New Delhi 110016, India, and
[2]Chemical Fibre Research Institute, China Textile University, Shanghai 200051, China

SYNOPSIS

A series of undrawn and drawn tapes has been prepared from HDPE, as well as, blends consisting of 90% HDPE and 10% ethylene copolymers. The influence of both the molecular irregularity of ethylene copolymers and resultant crystallization behavior on structure and mechanical properties of these blends has been investigated using differential scanning calorimetry, wide- and small-angle X-ray diffraction, mechanical response at small and large strains, and dynamic mechanical thermal analysis. The tensile drawing study of undrawn tapes shows enhanced strain hardening and a consistent reduction in natural, as well as, maximum achievable draw ratio with an increase in molecular irregularity of ethylene copolymers. It has been confirmed that blends are partially miscible in the amorphous, as well as, in the crystalline phase through cocrystallization. The lateral crystallite thicknesses, crystallinity, and amorphous phase orientation of blends consistently decreases with an increase in molecular irregularity of ethylene copolymers because of a large-scale change in crystallization and drawing behavior of HDPE component in the blends. There is a distinct possibility that the molecular network exerts an important influence on physical and mechanical properties of undrawn and drawn tapes. © 1996 John Wiley & Sons, Inc.

INTRODUCTION

In recent years, extensive studies have been carried out on ultra-oriented high-density polyethylene (HDPE) fibers with tensile moduli greater than 150 GPa and draw ratio exceeding 100.[1,2] However, only limited literature[3-6] is available on uniaxial deformation behavior of polyolefin blends with HDPE as the main component.[4-6] These studies are concerned with the maximum achievable draw ratio, optimum processing parameters, as well as, the degree of molecular orientation and the crystallographic character for producing improved mechanical properties of drawn materials.

In recent years, studies have also been carried out on structure-morphology and deformation behavior of fibers and films produced from various ethylene copolymers of varied branch densities.[7-16] It is well known that physical properties of these copolymers are very sensitive linear crystallizable segment lengths between the two consecutive branch points and the size of the side branches. These parameters influence the morphology of the amorphous phase, particularly the large increase in the fraction of amorphous phase. The other structural parameters notably affected are crystallization behavior, crystal fold length, lateral thicknesses of crystalline lamellae, degree of crystallinity, crystal defects, and melting temperatures.[7,12]

In this study an attempt is made to obtain qualitative relations between structural properties of undrawn and drawn HDPE/ethylene copolymer blends and physical properties. Particular emphasis is on the influence of molecular irregularity of ethylene copolymers on deformation behavior and the resultant mechanical properties of blends.

EXPERIMENTAL

Materials

Commercial grade HDPE, high-molecular-weight, high-density polyethylene (HMWPE), linear low-

* To whom correspondence should be addressed.

Journal of Applied Polymer Science, Vol. 60, 1517–1525 (1996)
 CCC 0021-8995/96/101517-09

density polyethylene (LLDPE), low-density polyethylene (LDPE), ethylene vinylacetate (EVA), and ethylene-propylene-diene terpolymer (EPDM) were used in this study. Some characteristics of these materials are given in Table I.

All samples, except for EVA and EPDM were characterized by ^{13}C-NMR spectroscopy and IR spectroscopy. The intensities measured from these materials were analyzed using literature assignments for determination of branch type and co-unit concentration.[17,18] In case of the EVA and EPDM copolymer samples, the co-unit compositions are taken from literature reports.[19,20] The results are summarized in Table I.

Sample Preparation

The drawn blended tapes of blend composition 90 : 10 by weight, HDPE with HMWPE, LLDPE, LDPE, EVA, and EPDM were prepared using Betol-1820 single-screw extruder of L/D ratio 20, with a slit die having width and thickness dimensions of 13 and 0.4 mm, respectively. The temperature profile used for extrusion was 160°C at the feed zone, 200°C at the compression zone, and 220°C at the metering zone and the die end. The screw speed was kept at 12 rpm. The extruded tapes were immediately quenched in a water bath maintained at 30°C and were drawn in sequence on a 750-mm-long hot plate maintained at 95°C with a draw ratio of about 10×. After drawing, the tapes were collected on a take-up bobbin with a speed of 10 m/min. The drawn tapes were in the range of 950–1000 denier (denier is the weight in grams of 9000 meters of tape). For study of undrawn tapes, the as-extruded tapes were collected immediately after quenching bath on a take-up bobbin with a speed of 1 m/min.

Density and Density Crystallinity

Density of undrawn tapes were measured on a Davenport density gradient column. The weight fraction of crystalline polymer [$X_{c\,(den)}$] was determined using crystalline and amorphous densities as 1.004 and 0.853 g/cm^3, respectively.[21]

Birefringence

Birefringence (Δn) of drawn tapes was measured on a Leitz polarizing microscope, with a Leitz–Wetzler tilting plate-type compensator.

Wide-Angle X-Ray Diffraction

Wide-angle X-ray diffraction (WAXD) studies were carried out for determination of interplanar spacing (d_{hkl}), average lateral crystallite thicknesses (D_{hkl}), and crystallite orientation factor (f_c), for drawn HDPE and blended tapes. A Philips X-ray generator equipped with a Philips fiber goniometer was used for this study. For visual comparison WAXD photographic patterns of some selected samples were also obtained.

Crystallite Size and Interplanar Spacing

The average lateral crystallite thicknesses were estimated using the Scherrer equation[22,23] from the broadening observed in WAXD patterns of powder samples recorded in 10–45° 2θ range at a scanning rate of 1°/min. The shape factor K of the Scherrer equation, which has been shown by Hindeleh and Johnson[23] to vary considerably on crystal structure and morphology, is assumed to be unity. The values of d_{hkl} for (200) and (020) reflections were calculated according to the standard procedure.[22]

Table I Characteristics of Materials Used

Polymer Type	Commercial Code	Supplier	MFI*	Density (g/cm^3)	Comonomer Type and Composition
HDPE	GF 7745F	PIL, India	0.7	0.945	1.8 CH_3/100 C
HMWPE	GF 7755	PIL, India	0.4	0.953	2.1 CH_3/100 C
LLDPE	Dowlex-2045E	Dow Chem, USA	1.0	0.920	3.2 CH_3/100 C (L-octene)
LDPE	Dowlex-200	Dow Chem, USA	0.9	0.920	3.6 Ch_3/100 C
EVA	Elvax-4210	DuPont, USA	0.8	0.928	4.7 mol % vinylacetate
EPDM	Nordel-1040	DuPont, USA	40†	0.560	75 mol % ethylene and 4 mol % diene

* ASTM D 1238/L.
† Moony viscosity 40, measured at ML 4 at 121°C.

Table II Degree of Crystallinity, Longitudinal Lamellae Thickness, Temperature for Onset of Crystallization, Peak Crystallization Temperature, and Mechanical Properties of Undrawn Tapes

Sample	$X_{c(den)}$ (%)	$L_{c(SAXS)}$ (Å)	T_{onset} (°C)	T_c (°C)	σ_y (MPa)	NDR	MDR
HDPE	63	118	119.8	117.9	21	8.7	11.5
10 HMWPE	66	98	119.1	117.4	23	7.6	12.5
10 LLDPE	62	92	118.3	116.8	19	4.8	10.0
10 LDPE	60	93	118.2	116.2	17	3.9	8.9
10 EVA	51	72	117.3	115.6	14	4.3	9.0
10 EPDM	50	67	117.7	115.9	12	3.5	8.1

Crystallite Orientation Factor

The f_c was estimated from the azimuthal intensity distribution of (200) and (020) reflections using Herman's method.[22]

Amorphous Phase Orientation Factor

The amorphous orientation factor (f_{am}), was determined using the Stein and Norris method[22] in a manner applied to polyethylene by Pezutti and Porter.[24]

Small-Angle X-Ray Scattering

Small-angle X-ray scattering (SAXS) patterns were obtained on a set-up comprising a rotating anode X-ray generator operating at 50 kV and 200 mA and fitted with a Rigaku Europe compact small-angle goniometer. The raw scattering data were corrected for slit smearing using the Schmidt and Height method[25] and Lorentz factor.[22] The long period (L_p) was estimated by applying Bragg's law to the scattering angle of the maximum intensity measured parallel to the tape axis. The lamellae size in chain direction [$L_{c(SAXS)}$], was obtained by multiplying L_p with fraction of density crystallinity.

Differential Scanning Calorimetry

Melting and crystallization behavior was followed through differential scanning calorimetry (DSC) measurements on a Perkin–Elmer DSC-7. Measurements were made with ~ 8-mg samples in the temperature range between 30 and 180°C at a scanning rate of 20°C/min.

The weight fraction crystalline polymer [$X_{c(dsc)}$], was determined using standard heat of fusion for HDPE as 293 J/g.[21,26] The maximum lamellae size in chain direction [$L_{c(dsc)}$] for blends was estimated using Thomson equation as applied to polyethylene by Wlochowicz and Eder.[27]

Mechanical Properties

Drawing behavior of undrawn tapes was studied on an Instron tensile tester with a constant strain rate of 1000%/min. Mechanical properties of drawn tapes were measured at 100%/min strain rate and a gauge length of 150 mm.

The dynamic mechanical thermal analysis of drawn tapes was carried out in a tensile mode using Rheovibron dynamic viscoelastometer with a frequency of 3.5 Hz in the temperature range of −130 to +130°C and heating rate of 3°C/min.

RESULTS AND DISCUSSION

The MFI, co-unit type, concentration, and other relevant characteristics of HDPE, HMWPE, and various ethylene copolymers are given in Table I. The blended tapes of HDPE with HMWPE, LLDPE, LDPE, EVA, and EPDM were prepared. We divide the total blend specimens into two sets: (a) low degree of molecular irregularity (HDPE with HMWPE and LLDPE) and (b) high degree of molecular irregularity (HDPE with LDPE, EVA, and EPDM). These are qualitatively expressed as molecular irregularity for further discussions.

UNDRAWN TAPES

Crystallization and Drawing Behavior of Undrawn Tapes

The data on crystallinity, lamellae size, temperature of onset of crystallization (T_{onset}), peak crystallization temperature (T_c), and the mechanical properties of undrawn tapes are given in Table II. In

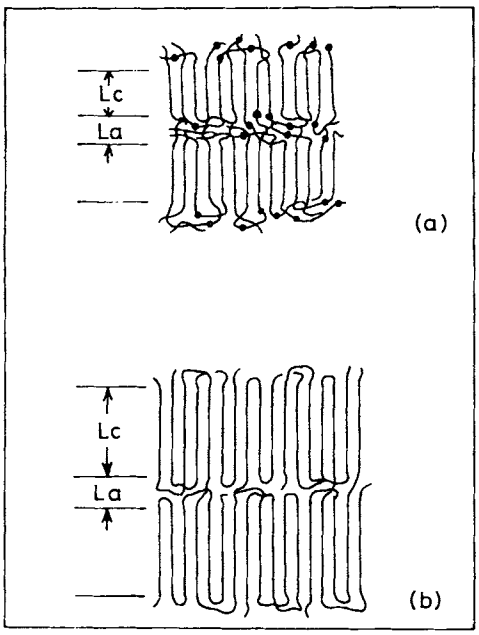

Figure 1 Schematic representation of the lamellar crystals (a) HDPE/ethylene copolymer blends and (b) linear polyethylene crystals. L_c, longitudinal crystallite thickness; L_a, interlamellar amorphous layer.

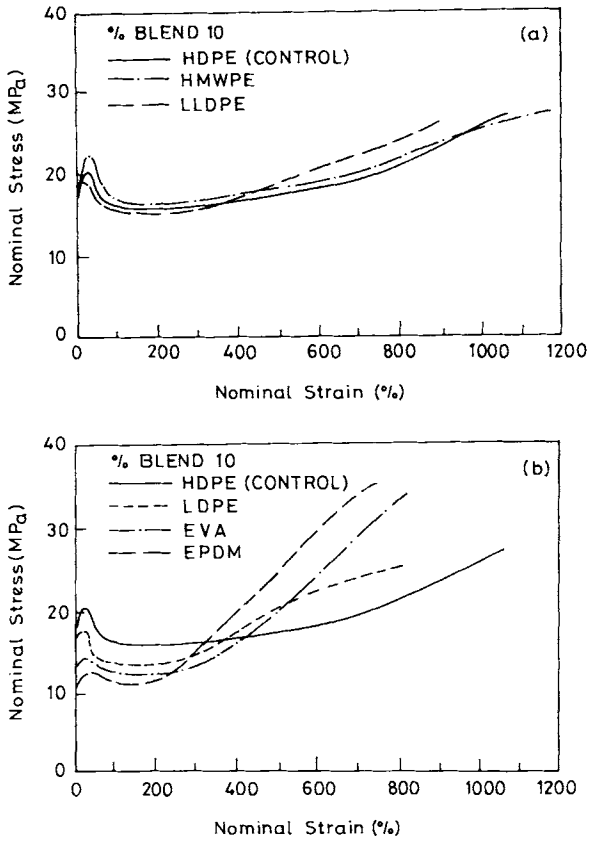

Figure 2 Load-extension curves of undrawn tapes of HDPE and its blends.

general, the degree of crystallinity and lamellae size decrease with the increasing molecular irregularity of ethylene copolymers. The addition of LDPE, EVA, and EPDM copolymers to HDPE reduced the crystallinity of blends from 63% for HDPE homopolymer to 60, 51, and 50% for the blends, respectively. Reduction is also observed for lamellae size determined from SAXS experiments. In addition to these structural changes, the rate of crystallization of HDPE is also decreased with the addition of copolymers as indicated by the shift of T_{onset} and T_c to lower temperatures. These results suggest that addition of ethylene copolymers to HDPE retarded the overall crystallization process in blends and decreased the crystallinity and lamellae size with the molecular irregularity of ethylene copolymers. The short ethylene segments and the noncrystallizable co-units of copolymer abandon the growing crystalline lamellae because these cannot be accommodated in the crystal lattice of polyethylene. Moreover, the rejected co-units of the copolymer at crystal–amorphous interface may further hinder the molecular mobility and hence the overall crystallization process.[12-16] This peculiarity of the crystallization and structure formation process of HDPE/ethylene copolymer blends leads to higher fraction of interlamellar tie molecules, denser molecular network, large crystal–amorphous interface, reduced crystallinity, and smaller lamellae size. A schematic representation of the structure of these blends is given in Figure 1.

Nominal stress–strain curves for as-extruded and partially oriented but undrawn tapes are given in Fig. 2, for two sets of blended samples. At low strains, it is seen from Figure 2 and Table II that yield stress (σ_y), decreases with an increase in molecular irregularity of second blend components. These results are consistent with the observed reduction in degree of crystallinity and lamellae size, which are known to exhibit a weaker resistance to onset of plastic deformation.[13-16]

The values of natural draw ratio (NDR) and maximum achievable draw ratio (MDR) are given in Table II. The values of NDR and MDR for HDPE, HDPE/HMWPE, and HDPE/LLDPE blends are larger, whereas blends prepared from LDPE, EVA, and EPDM components show a drastic reduction in NDR and MDR. In addition, the later blends also show a significant strain hardening during deformation of fibrous structure. The blending of LDPE, EVA, and EPDM copolymers to HDPE significantly increase the strain-hardening behavior of blends.

The phenomenon is attributed to the denser molecular network of these blends, which during drawing process reduces the molecular mobility and hence the natural and maximum draw ratio. An increase in strain hardening during post-neck deformation of fibrous structures, on the other hand, is associated with the increased fraction of interlamellar tie molecules, which enhances the resistance to longitudinal displacement of fibrils.[13-16,28,29]

DRAWN TAPES

Interplanar Spacing, Crystallite Thicknesses, and Crystallinity

The X-ray diffraction patterns of HDPE homopolymer and blends are illustrated in Figure 3, which shows that the characteristic features of WAXD patterns are quite similar for HDPE and blends. However, some changes in lateral crystallite thicknesses, interplanar spacings, and crystallinity are obtained. The relevant data are summarized in Table III.

The values of d_{hkl} for (200) and (020) reflections of HDPE match closely with reported literature.[22] These values, however, change significantly for LDPE, EVA, and EPDM blend systems. The interplanar spacing increases with increasing molecular irregularity of second blend components. This is attributed to the strain gradients generated in cocrystalline regions because of the variations in ethylene segment length of copolymer molecular chains.[8] Moreover, the high density of co-units at the crystal interface (basal planes) affects the molecular mobility and hence the spacing within crystal, particularly near the surface.[30] Such increase in interplanar spacing was reported earlier for various polyethylenes[7-11] and polyethylene/ethylene copolymer blends.[9-11]

The degree of crystallinity is decreased from 74% for HDPE homopolymer to 67, 60, and 65% for LDPE, EVA, and EPDM blends, respectively. Similar levels of reduction are also observed for lamellae thickness $L_{c\,(dsc)}$ and the lateral crystallite dimensions (Table III). These changes are related to the reduced molecular mobility in the melt and the limited number of sufficiently long ethylene sequences of the copolymer available for crystallization.

Melting Behavior

The DSC endothermic peaks for various blend systems were studied and the results are summarized in Table III. The peak melting temperature decreased from 135.4°C for HDPE homopolymer to 131.6, 132.4, and 132.4°C for LDPE, EVA, and EPDM blends, respectively. Another important observation relates to the broad single endothermic peak for all blends. The values of width of endothermic peaks at half height are given in Table III. The consistent lowering of T_m, presence of a single endothermic peak, and the broadening of melting endotherms with increasing molecular irregularity of blend components, may be related to the partial miscibility of two blend components in the amorphous phase, as well as, cocrystallization of blend components. The other parameters that may be indicative of such cocrystallization are the changes in interplanar spacings, reduction of crystallite dimensions, and the shift of T_{onset} and T_c to lower temperatures (Table II). The cocrystallization can be explained by considering that the crystallization of linear polyethylene, the first stage of the process, becomes the driving force for the crystallization of linear segments between the two consecutive co-units of the copolymer that are long enough to deposit on the growing substrate. A complete segregation of linear polyethylene and ethylene copolymer is therefore not possible.

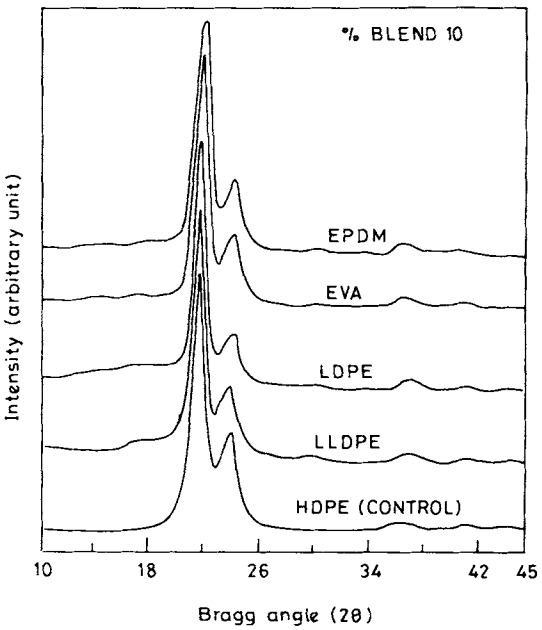

Figure 3 X-ray diffraction patterns of drawn tapes of HDPE and its blends.

Crystallite and Amorphous Phase Orientation

The values of f_c and f_{am} determined from WAXD studies are given in Table IV. The results show that

Table III Values of Interplanar Spacing, Lateral Crystallite Thickness, Lamellae Thickness, Degree of Crystallinity, Peak Temperature of Melting, and Width of Endothermic Peak at Half Height of Drawn Tapes

Samples	d_{hkl} (Å)		D_{hkl} (Å)		$L_{c(dsc)}$ (Å)	$X_{c(dsc)}$ (%)	T_m (°C)	ΔW (°C)
	$d_{(200)}$	$d_{(020)}$	$D_{(200)}$	$D_{(020)}$				
HDPE	3.725	2.468	101	139	272	74	135.4	5.5
10 HMWPE	3.727	2.478	106	127	253	71	134.9	5.8
10 LLDPE	3.749	2.482	97	132	189	68	132.6	5.9
10 LDPE	3.757	2.507	84	116	171	67	131.6	6.5
10 EVA	3.754	2.493	88	123	185	60	132.4	6.6
10 EPDM	3.749	2.509	93	119	185	65	132.4	7.1

for all blends, the values of f_c vary between 0.98 and 0.84; the values of f_{am} are, however, in the range of 0.57–0.31. It is also seen that f_{am} decreases with increasing molecular irregularity of second-blend components. These observations, therefore, indicate that the degree of amorphous phase orientation depends strongly on the structure of amorphous layers separating the lamellae. For blends containing relatively linear molecular chain ethylene copolymers with fewer co-units, such as LLDPE, the crystallization occurs nearly similarly to that of HDPE and HDPE/HMWPE blend. Thus, only small changes are expected in the drawing behavior. The drastic reduction in f_{am} for LDPE, EVA, and EPDM blends, on the other hand, can be attributed to (i) the denser molecular network, which restrict the viscoelastic flow of amorphous phase during drawing and (ii) the randomly oriented side branches that are expelled from the crystal lattice of PE into the amorphous phase.

Mechanical Properties

The values of breaking stress (σ_b), strain to break (ϵ_b), and initial modulus (E) for drawn tapes are summarized in Table IV. The breaking stress and modulus decrease from 480 MPa and 5.1 GPa for HDPE homopolymer tapes to 444, 417, and 411 MPa, and 4.2, 4.1, and 3.6 GPa for blends prepared from LDPE, EVA and EPDM blend components, respectively. This effect is attributed to the gradual decrease of f_{am}, f_c, and X_c with increasing molecular irregularity of second-blend components.

In Figure 4, breaking stress and modulus are plotted against the amorphous phase orientation of drawn tapes. The reduction in breaking stress and initial modulus with increasing molecular irregularity of second-blend component and with a decrease of f_{am}, particularly for LDPE, EVA, and EPDM blends is related to the reduced capability of these specimens to develop a highly oriented and fine fibrillar structure under uniaxial drawing. This is in agreement with the lower drawability and stronger strain-hardening effect observed during deformation of undrawn tapes. The marginal increase in breaking stress from 480 MPa for HDPE to 490 MPa; on the other hand, the initial modulus from 5.1 GPa for HDPE homopolymer tapes to 5.4 GPa for HDPE/HMWPE blended tapes is related to higher amorphous phase orientation and the presence of HMWPE molecules in the blend, which has a higher probability to form intercrystalline tie molecules.[31,32]

The room temperature stress–strain curves for drawn tapes are compared in Figure 5. The two sets of curves show very similar general features. The gradual increase in ductile behavior and lowering of yield stress with co-unit concentration of ethylene copolymers is related to the lower f_{am} and X_c. In contrast, the relatively higher yield stress and the concomitant reduction in breaking strain observed for HMWPE and LLDPE blends is attributed to the higher level of f_{am} and X_c.

Table IV Crystallite Orientation Factor, Amorphous Orientation Factor, and Mechanical Properties of Drawn Tapes

Sample	f_c	f_{am}	σ_b (MPa)	E (GPa)	ϵ_b
HDPE	0.98	0.50	480	5.1	0.27
10 HMWPE	0.98	0.57	490	5.4	0.23
10 LLDPE	0.98	0.48	473	4.9	0.31
10 LDPE	0.91	0.43	444	4.2	0.27
10 EVA	0.87	0.39	417	4.1	0.30
10 EPDM	0.84	0.31	411	3.6	0.34

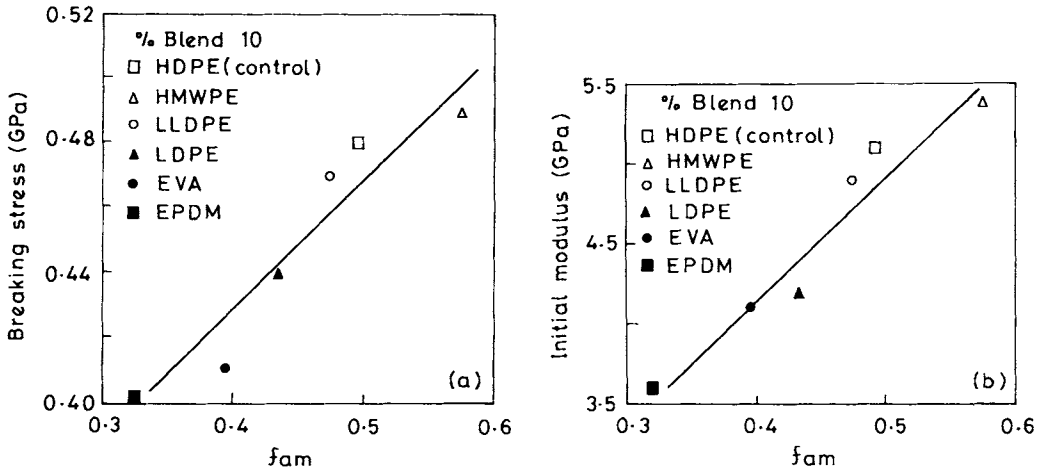

Figure 4 Amorphous phase orientation dependence of (a) breaking stress and (b) initial modulus for drawn tapes.

Dynamic Mechanical Behavior

In Figure 6 loss tangent (tan δ) is plotted as a function of temperature for various blends studied. Table V lists the temperature of main relaxations, whereas the results are depicted in Figure 6. HDPE and blends give three prominent relaxation peaks in the vicinity of −120, −30, and 95°C. First two transitions relate to the rubbery phase transition of HDPE. This is in agreement with the literature data on HDPE relaxation behavior.[33–37] The 10 HMWPE tapes also show similar mechanical behavior with a broader transition at around −35°C. In case of 10 LLDPE, 10 EVA, and 10 EPDM blends, however, a large shift in β-transition temperature (T_β), is observed. These blends show a transition in temperature range of −55 and −60°C, which is about 25 to 30°C lower than HDPE homopolymer. This may occur as a result of the increased fraction of the amorphous phase and the decrease in activation energy needed for the motions of disordered chain units, loose folds, and rejected co-units from the crystal lattice of polyethylene.

The α-transition associated with the transitional motions of segments in the crystalline phase and crystal–amorphous interfacial zone of polyethylene[33–36] is seen between 30 and 110°C. The peak temperature of this transition ($T_{\alpha c}$) gradually shifts to lower temperatures with increasing molecular irregularity of ethylene copolymer blend component. The $T_{\alpha c}$ of HDPE is in the vicinity of 93°C. For 10 LLDPE, 10 EVA, and 10 EPDM blends the $T_{\alpha c}$ decreases to 88, 80, and 78°C, respectively. This is in agreement with the observed crystalline structure and morphology of these

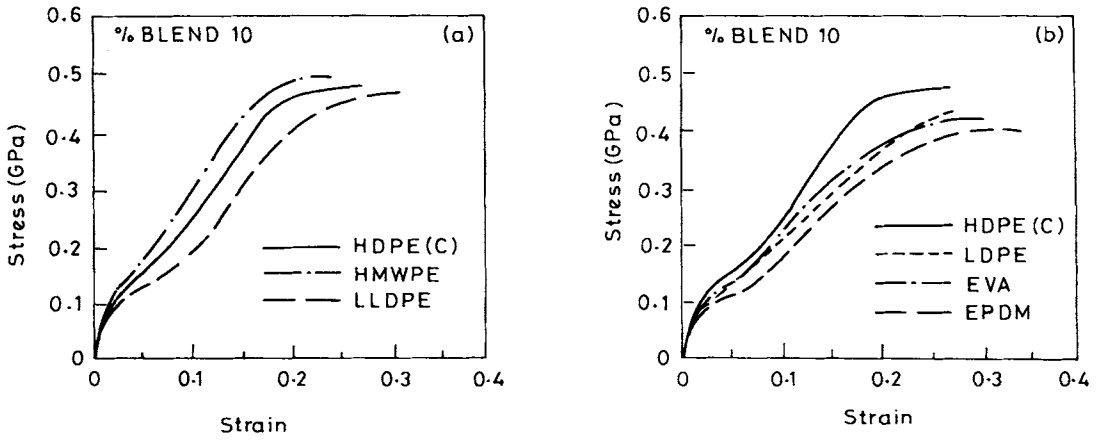

Figure 5 Stress–strain plots of drawn tapes for HDPE and its blends.

blends and is related to (i) a decrease in crystallinity and average crystal thickness and (ii) formation of imperfect crystallites associated with the cocrystallization of blend components.

CONCLUSIONS

The crystallization behavior and structure-morphology of high-density linear polyethylene is altered markedly by blending a comparatively small amount of ethylene copolymers. Cocrystallization among the two blend components is supported from DSC and X-ray analysis, in which a consistent depression in melting temperature, delayed crystallization, reduction in crystallinity and crystallite dimensions, and a small increase in interplanar spacing with increasing molecular irregularity of blend components was observed.

The mechanical properties of drawn blended tapes showed a consistent reduction in breaking stress and initial modulus, with an increasing degree of branching in ethylene copolymers. On the contrary, the elongation to break shows the opposite trend. This suggests that it should be possible to modify high-density linear polyethylene with properties tailored to a desired specification by choosing suitable grades of ethylene copolymers and blending them with linear polyethylene to predetermined proportions.

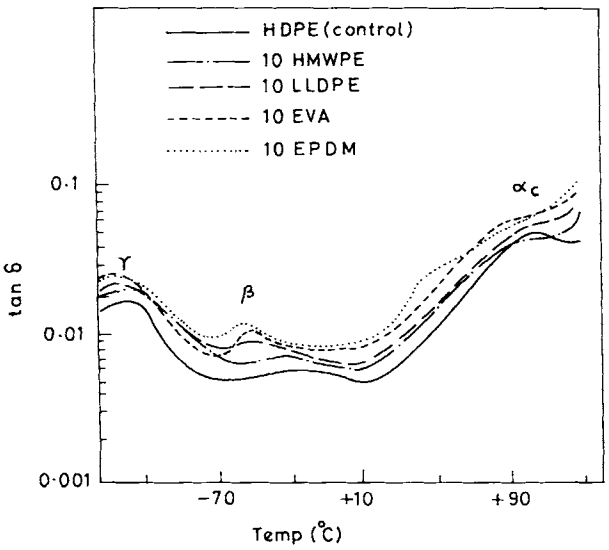

Figure 6 Temperature dependence of the loss tangent for drawn tapes.

Table V Temperature of α, β, and γ Relaxations of Drawn Tapes

Sample	T_γ (°C)	T_β (°C)	$T_{\alpha c}$ (°C)
HDPE	−114	−30	93
10 HMWPE	−118	−35	88
10 LLDPE	−118	−56	88
10 EVA	−120	−54	80
10 EPDM	−120	−57	78

REFERENCES

1. W. T. Mead, C. S. Desper, and R. S. Porter, *J. Polym. Sci., Polym. Phys. Ed.*, **17**, 859 (1979).
2. G. Capaccio, T. A. Crompton, and I. M. Ward, *J. Polym. Sci., Polym. Phys. Ed.*, **14**, 1641 (1976).
3. H. W. Kammer, C. Kummerloewe, R. Greco, C. Mancarella, and E. Martuscelli, *Polymer*, **29**, 963 (1988).
4. R. D. Deanin and M. F. Sansone, *Polym. Prepr., Amer. Chem. Soc. Div. Polym. Chem.*, **19**(1), 211 (1978).
5. G. A. Gallagher, R. Jakeways, and I. M. Ward, *J. Appl. Polym. Sci.*, **43**, 1399 (1991).
6. R. Greco, G. Mucciariello, G. Ragosta, and E. Martuscelli, *J. Mater. Sci.*, **15**, 845 (1980).
7. E. Martuscelli, *J. Macromol. Sci., Phys.*, **B11**, 1 (1975).
8. E. Krenzer and W. Ruland, *Colloid Polym. Sci.*, **259**, 405 (1981).
9. G. H. Edward, *Br. Polym. J.*, **18**, 88 (1986).
10. P. Vadhar and T. Kyu, *Polym. Eng. Sci.*, **27**, 202 (1987).
11. H. W. Starkweather, *J. Appl. Polym. Sci.*, **25**, 139 (1980).
12. R. Alamo, R. Domszy, and L. Mandelkern, *J. Phys. Chem.*, **88**, 6587 (1984).
13. R. Seguela and F. Rietsch, *Polymer*, **27**, 703 (1986).
14. R. Seguela and F. Rietsch, *Eur. Polym. J.*, **20**, 765 (1984).
15. G. Capaccio and I. M. Ward, *J. Polym. Sci., Polym. Phys. Ed.*, **22**, 475 (1984).
16. G. Meinel and A. Peterlin, *Eur. Polym. J.*, **7**, 657 (1971).
17. S. K. Rana, *Crystallization Behaviour and Structure Property Correlation of High-Density Polyethylene/Linear-Low-Density Polyethylene Blends,"* Ph.D. Thesis, Indian Institute of Technology, Delhi, July 1992.
18. Ser van der Ven, *Polypropylene and Other Polyolefins—Polymerization and Characterization*, Elsevier, Amsterdam, 1990, p. 447, 535.
19. Technical Information Brochure No. A95645. E. I. du Pont de Nemours and Company, USA.
20. B. K. Ratnam, *Modification of Polypropylene with Elastomers and Glass Fibres*, Ph.D. Thesis, Indian Institute of Technology, Delhi, July 1992.

21. R. P. Runt, in *Encyclopedia of Polymer Science and Engineering,* Vol. 4, 2nd ed., H. F. Mark, N. M. Bikales, C. G. Overberger and G. Menges, Eds., Wiley-Interscience, New York, 1986, p. 482.
22. L. E. Alexander, *X-ray Diffraction Methods in Polymer Science,* Krieger Press, New York, 1979.
23. A. M. Hindeleh and D. J. Johnson, *Polymer,* **19,** 27 (1978).
24. J. L. Pezutti and R. S. Porter, *J. Appl. Polym. Sci.,* **30,** 4251 (1985).
25. P. W. Schmidt and R. Height, Jr., *Acta Cryst.,* **17,** 138 (1960).
26. A. K. Gupta, S. K. Rana, and B. L. Deopura, *J. Appl. Polym. Sci.,* **44,** 719 (1992).
27. A. Wlochowicz and M. Eder, *Polymer,* **25,** 1268 (1984).
28. G. Capaccio and I. M. Ward, *Polymer,* **16,** 239 (1975).
29. G. Capaccio, T. A. Crompton, and I. M. Ward, *J. Polym. Sci., Polym. Phys. Ed.,* **18,** 301 (1980).
30. L. Mandelkern, M. Glotin, and R. S. Benson, *Macromolecules,* **14,** 22 (1981).
31. B. L. Deopura and S. Kadam, *J. Appl. Polym. Sci.,* **31,** 2145 (1986).
32. S. J. Mahajan, K. Bhoumik, and B. L. Deopura, *J. Appl. Polym. Sci.,* **43,** 49 (1991).
33. R. Popli, M. Glotin, L. Mandelkern, and R. S. Benson, *J. Polym. Sci., Polym. Phys. Ed.,* **22,** 407 (1984).
34. S. D. Clas, D. C. McFaddin, and K. E. Russell, *J. Polym. Sci., Polym. Phys. Ed.,* **25,** 1057 (1987).
35. Y. P. Khanna, E. A. Turi, T. J. Taylor, V. V. Vickroy, and R. F. Abott, *Macromolecules,* **18,** 1302 (1985).
36. C. Jourdan, J. Y. Cavaille, and J. Perez, *J. Polym. Sci., Polym. Phys. Ed.,* **27,** 2361 (1989).
37. S. R. Hu, T. Kyu, and R. S. Stein, *J. Polym. Sci., Polym. Phys. Ed.,* **25,** 71 (1987).

Received June 16, 1994
Accepted October 7, 1995